NATIONAL ADVISORY COMMITTEE FOR AERONAUTICS

TECHNICAL NOTE

NO. 1687

JET DIFFUSER FOR SIMULATING RAM-PRESSURE AND ALTITUDE

CONDITIONS ON A TURBOJET-ENGINE STATIC TEST STAND

By Robert H. Essig, H. R. Bohanon and David S. Gabriel

Flight Propulsion Research Laboratory
Cleveland, Ohio

Washington
August 1948

NATIONAL ADVISORY COMMITTEE FOR AERONAUTICS

TECHNICAL NOTE NO. 1687

JET DIFFUSER FOR SIMULATING RAM-PRESSURE AND ALTITUDE

CONDITIONS ON A TURBOJET-ENGINE STATIC TEST STAND

By Robert H. Essig, H. R. Bohanon
and David S. Gabriel

SUMMARY

An investigation has been made of a jet diffuser designed to utilize the kinetic energy of the jet from a turbojet engine to reduce the discharge pressure at the exhaust nozzle and thereby to provide simulated ram-pressure ratios across the engine and altitudes. The jet diffuser, designed for use with a turbojet engine having a $12\frac{1}{2}$-inch-diameter exhaust nozzle, consists of an exhaust chamber, a diffuser-inlet nozzle, a straight 10-inch-long throat, and a diffuser section followed by a 4-foot straight duct. At any engine speed, the pressure in the exhaust chamber may be regulated by a variable-area shutter at the diffuser outlet.

Curves of performance data for a turbojet engine at several ram-pressure ratios show the range of engine operating conditions obtainable with the jet diffuser.

A maximum engine-inlet to exhaust-chamber pressure ratio (simulated ram-pressure ratio) of about 2.4 was obtained at a simulated pressure altitude of approximately 23,000 feet. The experimental and calculated pressure rises between the exhaust chamber and diffuser throat were in good agreement. Comparison of the engine thrust obtained at a ram-pressure ratio of 1.0 with and without the jet diffuser indicated that the presence of the diffuser did not interfere with the gas flow through the engine-exhaust-nozzle outlet at this ram-pressure ratio. Data from pressure surveys in the exhaust chamber indicated that the presence of the jet diffuser did not interfere with the gas flow at ram-pressure ratios greater than 1.0

INTRODUCTION

Two of the operating conditions affecting the performance of turbojet engines are altitude and ram-pressure ratio (ratio of

compressor-inlet total pressure to ambient atmospheric pressure).
The results of reference 1, which reports a theoretical analysis
(supported by experimental data) of the effect of altitude on the
performance of turbojet engines, show that, with the exception of
parameters involving fuel flow, the performance variation of turbo-
jet engines with altitude for any constant ram-pressure ratio can
be correlated by the use of reduction factors. The effects of ram-
pressure ratio, however, cannot be correlated by the reduction
factors. Consequently, it has been necessary to resort to either
wind-tunnel or flight studies to determine the performance of
turbojet engines under ram conditions.

A jet diffuser that can be used to simulate ram-pressure
conditions on a static test stand was developed at the NACA
Cleveland laboratory to reduce the extensive amount of equipment
required for runs under ram or flight conditions. Preliminary
results of the earlier phase of this investigation were presented
in an NACA release by H. R. Bohanon, David S. Gabriel, and Robert
H. Essig in November 1946. The present report supersedes this
preliminary publication and incorporates a more complete descrip-
tion and analysis of the performance of the jet diffuser. Applica-
tion of the jet diffuser is illustrated by engine-performance data
obtained over a range of engine rotor speeds from about 82 to
100 percent of maximum engine speed and for ram-pressure ratios
as high as approximately 2.4. The engine-performance data at a
ram-pressure ratio of 1.0 are compared with data taken without the
jet diffuser. Pressure surveys in the diffuser exhaust chamber
are included to show whether the presence of the jet diffuser
interferes with the gas flow from the engine exhaust nozzle and
to verify the accuracy of the thrust calibration.

DESCRIPTION OF JET DIFFUSER

The jet diffuser utilizes the kinetic energy of the exhaust
jet from the turbojet engine to reduce the engine back pressure
and thereby to create a pressure ratio between the compressor
inlet and the engine outlet that simulates a ram-pressure ratio.
Because the engine exhausts into a pressure lower than sea-level
atmospheric, the simulated ram-pressure ratio is obtained at a
simulated pressure altitude corresponding to the engine exhaust
pressure. Reference 1 shows that the performance at the various
simulated pressure altitudes resulting from the decreased exhaust-
chamber pressures can be correlated by plotting the engine per-
formance in terms of generalized parameters; hence, the effects
of ram-pressure ratio and altitude on performance may be separated.

The jet diffuser (fig. 1), which was designed for use on a turbojet engine having a $12\frac{1}{2}$-inch-diameter exhaust nozzle, consists of a cylindrical exhaust chamber, an inlet nozzle, a 10-inch-long straight throat, and a diffuser section followed by a 4-foot-long straight duct that is fitted with a movable sleeve-type shutter and a conical target.

Two different diffuser-inlet nozzles and throat configurations were used. The first configuration, which is shown dimensioned in figure 1, consisted of a bell-shaped inlet nozzle and a $13\frac{1}{2}$-inch-diameter throat (about $16\frac{1}{2}$ percent greater area than the area of the engine-exhaust-nozzle outlet); the second configuration consisted of a conical inlet nozzle and a 14-inch-diameter throat (about $25\frac{1}{2}$ percent greater area than the area of the engine-exhaust-nozzle outlet).

The diffuser proper was constructed with a 7° total angle of diffusion (area ratio of 3.4 for the $13\frac{1}{2}$-in.-diameter throat and 3.3 for the 14-in.-diameter throat) and was 93 inches long.

The exhaust chamber at the inlet to the jet diffuser provided a region of constant pressure that facilitated the measurement of ambient engine-exhaust pressure (exhaust-chamber pressure) and permitted the reproduction of actual engine performance using the standard engine exhaust.

The movable-shutter arrangement and the conical target were used to adjust the exhaust-chamber pressure, and thus the ram-pressure ratio across the engine, at various engine speeds. A hydraulically operated piston with a 12-inch stroke was used to change the shutter position. The sleeve-type shutter assembly, which moved parallel to the diffuser axis, was used to eliminate the forces other than friction acting on the control valve, and the saw-toothed edge of the shutter permitted fine adjustment of the exhaust-chamber pressure.

The entire diffuser assembly was mounted on a movable frame, as shown in figure 2. This movable diffuser frame provided a means of adjusting the diffuser position with respect to the exhaust-nozzle outlet, which, for this investigation, was located approximately $8\frac{3}{4}$ inches from the diffuser-throat inlet (fig. 1).

During the runs, the exhaust chamber was flexibly connected to the
engine by a clamped rubber diaphragm seal, as shown in figure 3,
and the movable diffuser frame was rigidly fastened to the concrete
test-cell apron. A radiation shield was installed inside the
exhaust chamber to protect the diaphragm from damage by heat. Both
inner and outer diaphragm-clamping flanges were cooled by water
coils, and a water spray was directed against the outer face of the
diaphragm.

INSTALLATION AND INSTRUMENTATION

Installation. - Jet-diffuser performance was investigated with
a 1600-pound-thrust, centrifugal-compressor-type turbojet engine.
Figure 4 is a schematic diagram of the setup showing the test cell,
the engine mounting frame, the thrust-measuring-device linkage, and
the jet diffuser. The engine was mounted on a rigid frame, which
was suspended from the cell roof by four ball-bearing pivoted rods.
Lateral movement of the engine frame was prevented by ball-bearing
guide rollers. The tail pipe, which was fitted with a $12\frac{1}{2}$-inch-

diameter exhaust nozzle, extended through an air seal (detail A,
fig. 4) in the outer cell wall.

Instrumentation. - The thrust forces produced by the engine
were indicated by the measured pressures in a calibrated balanced-
diaphragm air cell connected to the engine frame by a bell-crank
linkage. Details of the thrust calibration are subsequently dis-
cussed. All supply lines and instrument connections to the engine
were flexible in order that the restraining forces on the free-
swinging frame would be minimized.

Engine fuel (kerosene) flow was measured with a calibrated
rotameter and engine rotor speed was measured with a chronometric
tachometer.

The air supply to the engine entered the nearly airtight test
cell through a standard A.S.M.E. air-metering nozzle with a throat
diameter of 18 inches (fig. 4). An air-supply diffuser, which has
an area ratio of 4, was connected to the A.S.M.E. nozzle in order
to convert the velocity pressure in the nozzle throat to static
pressure in the test cell.

The following pressure and temperature measurements, located
as shown in figures 1, 3, and 4, were made:

(a) Compressor-inlet air temperature T_1, average of four
open-type thermocouples in inlet to engine cowl

(b) Compressor-inlet total pressure P_1, one open-end tube in test cell

(c) Tail-pipe indicated gas temperature (assumed to be total temperature) T_7, average from five strut-type thermocouples located in tail pipe 8 inches upstream of exhaust nozzle

(d) Exhaust-chamber static pressure p_8, piezometer ring with four wall taps equally spaced around exhaust-chamber wall approximately in plane of engine-exhaust-nozzle outlet. This pressure corresponds to simulated-altitude ambient pressure. The reading of the piezometer ring was independently checked with a single exhaust-chamber wall tap connected to a separate manometer.

(e) Jet-diffuser-throat static pressure p_9, single wall tap located 1 inch upstream of throat outlet

(f) Diffuser-outlet static pressure p_{10}, single wall tap located at outlet of 7° diffuser section

In addition, the following pressure surveys were made:

(a) Static pressures at various locations along jet-diffuser-inlet nozzle, throat, and diffusing sections (figs. 1 and 3)

(b) Exhaust-chamber static pressures along exhaust-chamber wall, along engine exhaust nozzle, and radially across flexible diaphragm (fig. 3)

PROCEDURE

With the bell-shaped diffuser-inlet nozzle and the $13\frac{1}{2}$-inch-diameter throat, engine runs were made over a range of rotor speeds from about 13,600 to 16,600 rpm (82 to slightly over 100 percent of rated engine speed) for seven diffuser-outlet shutter positions. Shutter positions are designated A to G, where A is the wide-open position (maximum ram-pressure ratio) and G is the nearly closed position (ram-pressure ratio about 1.0). The various shutter positions were arbitrarily chosen to divide the range of ram-pressure ratios obtained at top speed into approximately equal increments.

Engine runs were also made with the conical inlet nozzle and a 14-inch-diameter throat over a range of rotor speeds from 13,600 to 16,600 rpm for four diffuser-outlet shutter positions.

The runs with these two configurations provided data to investigate the effect of the jet-diffuser inlet-nozzle shape on the engine thrust. Data were also obtained during these runs to investigate the effect of diffuser-throat area on the performance of the jet diffuser.

Because the effective area of the exhaust-chamber diaphragm was large, the forces on the engine due to the difference between the exhaust-chamber pressure and the atmospheric pressure were of the same order of magnitude as the jet thrust produced by the engine. In order to permit measurement of the jet thrust produced by the engine at different exhaust-chamber pressures, a dead-weight thrust calibration was made with zero gas flow through the engine. The calibration was made at several different pressures, which were obtained by blanking off the engine tail pipe and the diffuser outlet and evacuating the exhaust chamber with a vacuum pump.

The possibility that the presence of the walls of the jet diffuser may affect the engine thrust was investigated by measuring the static pressures at various locations in the exhaust chamber during the runs. Because the effective pressure acting on the diaphragm seal between the exhaust chamber and the engine tail pipe was also determined from the pressure surveys, these measurements also constituted a check on the accuracy of the pressure used for the calibration of the balanced-diaphragm thrust-measuring device.

Runs were also made without the jet diffuser to establish standard engine performance at a ram-pressure ratio of 1.0.

SYMBOLS

The following symbols are used in this report:

A   area, (sq ft)

A_n engine exhaust-nozzle-outlet area, (sq ft)

F   exhaust-jet thrust (total mass flow of exhaust gas × effective exhaust-jet velocity), (lb)

g   dimensional constant, 32.2 (ft/sec^2)

M   local Mach number

N   engine speed, (rpm)

P   total pressure, (lb)/(sq ft absolute)

p   static pressure, (lb)/(sq ft absolute)

R   gas constant, 53.4 (ft-lb)/(lb)(^{O}R)

T   total temperature, (^{O}R)

t   static temperature, (^{O}R)

V   velocity, (ft/sec)

W_a air flow, (lb/sec)

W_f fuel flow, (lb/hr)

W_t air flow plus fuel flow, (lb/sec)

γ ratio of specific heats of exhaust gas, 1.33

η diffuser efficiency

ρ density, (lb/cu ft)

Subscripts:

1   compressor inlet

7   tail pipe

8   exhaust chamber

9   outlet of diffuser throat

10   outlet of diffuser proper

j   conditions of jet after complete expansion to ambient altitude
        pressure p_8

METHOD OF CORRECTION OF ENGINE-PERFORMANCE DATA

Reference 1 shows that the performance of a turbojet engine in flight may be correlated for any constant ram-pressure ratio independently of altitude by means of reduction factors similar to the following:

$$\delta = \frac{\text{exhaust-chamber static pressure} \quad p_8}{\text{NACA standard sea-level pressure}}$$

$$\theta = \frac{\text{compressor-inlet temperature} \quad T_1}{\text{NACA standard sea-level temperature}}$$

In some performance investigations of turbojet engines, the compressor-inlet total pressure rather than the exhaust static pressure is used in defining δ. The definition of δ based on the exhaust static pressure is used because a more complete separation of the effects of ram and altitude is thus effected.

The reduction factors δ and θ used to generalize the performance variables neglect any changes that may occur in the combustion efficiency. Therefore, extrapolation of the experimental results involving the fuel consumption of the engine to high altitudes may be unreliable. The variation of combustion efficiencies, and hence the error of correlation, may be expected to be small at low altitudes but would increase as the burner critical altitude is approached.

The performance data at various altitudes are correlated by plotting the results in terms of the following generalized parameters:

F_j/δ corrected jet thrust

$N/\sqrt{\theta}$ corrected engine speed

P_1/p_8 simulated ram-pressure ratio

T/θ corrected total temperature

$W_a\sqrt{\theta}/\delta$ corrected air flow

$W_f/\delta\sqrt{\theta}$ corrected fuel flow

The jet thrust represents the product of the mass flow of exhaust gas and the effective jet velocity. The product of the mass flow of air into the engine and the airplane speed must be subtracted to compute the net thrust for flight conditions.

RESULTS AND DISCUSSION

Operating Characteristics of Jet Diffuser

The variation of exhaust-chamber pressure with engine speed for various shutter positions is shown in figure 5 for the bell-shaped inlet nozzle and a $13\frac{1}{2}$-inch-diameter diffuser throat. These curves illustrate the range of exhaust-chamber pressures, and hence ram-pressure ratios, obtainable. The exhaust-chamber absolute pressure decreased with an increase in engine speed for all shutter positions B to G and increased at each constant engine speed as the shutter was closed. With the diffuser shutter wide open (position A), the exhaust-chamber pressure reached a minimum of 12.5 inches of mercury absolute at an engine speed of about 16,100 rpm. This value corresponds to a ram-pressure ratio of 2.33 at a standard pressure altitude of approximately 22,000 feet. Although not shown in figure 5, increasing the diffuser-throat diameter to 14 inches decreased the minimum exhaust-chamber pressure obtainable to 12.1 inches of mercury absolute at an engine speed of about 16,200 rpm, and hence extended the range of available ram-pressure ratios to 2.43 at a standard pressure altitude of approximately 23,000 feet. The occurrence of the minimum exhaust-chamber pressure at less than maximum engine speed indicates choking (a limiting Mach number) in the diffuser throat. Choking could be eliminated by use of a larger diffuser-throat area but the data for the two throat sizes investigated show that the result would be a shifting of the curve for wide-open shutter to the right on figure 5 with a subsequent decrease in the ram-pressure ratios obtainable at lower engine speeds.

The over-all pressure rise between the exhaust-chamber pressure and the diffuser-outlet pressure (atmospheric pressure) was the sum of a pressure rise between the exhaust chamber and the diffuser-throat outlet due to the abrupt increase in flow area (sudden expansion) and a pressure rise in the divergent diffuser section. Data were obtained for an analysis of these two pressure-rise processes by measuring static wall pressures along the exhaust chamber, the diffuser-inlet nozzle and throat, and along the divergent diffuser. A plot of these static wall pressures is shown in figure 6 for the bell-shaped diffuser-inlet nozzle and $13\frac{1}{2}$-inch-diameter throat for several engine speeds at the wide-open-shutter position (position A). The pressure rise between the exhaust chamber and the diffuser-throat outlet is appreciable for all engine speeds. At the two highest engine speeds, however, the

pressure distribution is complicated by the presence of shock waves.
The dashed lines indicate the regions of uncertain pressure measure-
ments. The pressure along the length of the exhaust chamber is
constant and the pressures in the diffuser-inlet nozzle and throat
are variable.

An analytical investigation of the pressure rise between sta-
tions 8 and 9 was made to investigate the nature of the process
and determine whether an optimum diffuser-throat area exists. The
analysis was made by combining the fundamental equations of con-
servation of energy, momentum, and mass flow and the gas law to
give the following equation:

$$\frac{F_j}{\gamma p_8 A_n} = \frac{1 + \frac{2}{\gamma-1}\frac{p_9}{p_8} - \frac{\gamma+1}{\gamma-1}\left(\frac{p_9}{p_8}\right)^2}{\frac{2\gamma^2}{\gamma-1}\left(\frac{A_n}{A_9}\right)^2 - 2\gamma\frac{A_n}{A_9} - \frac{2\gamma}{\gamma-1}\frac{p_9}{p_8}\frac{A_n}{A_9}} \tag{1}$$

The detailed derivation of equation (1) is given in the appendix.

This equation expresses the relation between the jet thrust
produced by the engine F_j, the ratio of exhaust-nozzle-outlet
area to diffuser-throat area A_n/A_9, and the ratio of pressure at
the diffuser-throat outlet to pressure at the exhaust chamber p_9/p_8.
For given diffuser-throat and exhaust-nozzle-outlet areas, the
pressure ratio p_9/p_8 is a function only of the ratio F_j/p_8.

The variation of the pressure ratio p_9/p_8 with the fac-
tor $F_j/\gamma p_8 A_n$, which is equivalent to the square of the exhaust-
gas Mach number, is shown in figure 7 for both calculated and
experimental values. The calculated curve was obtained from
equation (1). The experimental values of pressure ratio approach
the ideal (calculated) curve very closely at low values of the
parameter $F_j/\gamma p_8 A_n$ but are only about 80 percent of the ideal
at high values of the parameter. This difference is attributed
largely to friction and separation losses. Good correlation of
the data for various shutter positions is obtained with the excep-
tion of the two points at the extremely high values of jet velocity.
The agreement between the calculated and experimental data for the
14-inch-diameter throat, not shown, was similar.

678

The dependence of the pressure rise between the exhaust chamber and the diffuser throat on the parameter $F_j/\gamma p_8 A_n$ and the area ratio (equation (1)) indicates that for a given value of the parameter an optimum area ratio A_n/A_9 may exist. This optimum area ratio is also a function of the efficiency and the area ratio of the diffuser proper.

The existence of an optimum diffuser-throat area for any value of $F_j/\gamma p_8 A_n$ is confirmed by the experimental data for the two area ratios A_n/A_9 shown in figure 8. The curves for the area ratios cross at a value of $F_j/\gamma p_8 A_n$ of 1.95 indicating that an optimum area ratio, lying between the two area ratios investigated, exists for this value of $F_j/\gamma p_8 A_n$.

A plot of the efficiency of the diffuser proper (from throat outlet to station 10) with the $13\frac{1}{2}$-inch-diameter throat is given in figure 9 as a function of the factor $F_j/\gamma p_8 A_n$ for the wide-open shutter position. The following equation defines the diffuser efficiency:

$$\eta = \frac{2g \dfrac{\gamma}{\gamma-1} Rt_9 \left[\left(\dfrac{p_{10}}{p_9}\right)^{\frac{\gamma-1}{\gamma}} - 1\right]}{V_9^2 - V_{10}^2} \tag{2}$$

For this calculation, the static temperature in the diffuser t_9 was obtained from the total temperature T_9, which was assumed to be equal to the tail-pipe total temperature T_7. The diffuser efficiency at a low value of $F_j/\gamma p_8 A_n$ is about 85 percent, but falls off at high values of $F_j/\gamma p_8 A_n$ to about 83 percent.

Engine Performance

The use of the jet diffuser for simulating ram-pressure conditions is illustrated by figures 10 to 13, which show the corrected performance of the engine plotted against ram-pressure ratio for various corrected engine speeds. The corrected performance parameters plotted are jet thrust, air flow, fuel flow, and tail-pipe

gas temperature. The data were adjusted for slight experimental differences in engine speed by plotting the rough data of the engine performance against speed for various ram-pressure ratios and then adjusting the parameters to a constant engine speed.

The data points for runs with both the $13\frac{1}{2}$-inch- and 14-inch-diameter throats are included in figures 10 to 13 and fall on common curves. This agreement indicates that throat size and the shape of the diffuser-inlet nozzle (conical or bell-shaped) do not influence the engine operating characteristics. The extension of the range of ram-pressure ratios obtainable at high engine speeds when the 14-inch throat having a conical inlet nozzle is used is due to the effect of diffuser-throat area previously discussed.

Cross plots of figures 10 to 13 are presented in figures 14 to 17, in which the corrected engine performance is shown as a function of the corrected engine speed for various ram-pressure ratios from 1.0 to 2.2. The limited range of engine speeds that can be obtained with the jet diffuser at ram-pressure ratios above about 1.4 is evident from these curves. The points on each figure, which are performance data at a ram-pressure ratio of 1.0 taken without the jet diffuser, show good agreement with the cross-plotted curves. This agreement indicates that the jet diffuser does not interfere with the flow through the engine exhaust nozzle at a ram-pressure ratio of 1.0. At ram-pressure ratios high enough to produce critical pressure ratios across the engine exhaust nozzle, it is reasonable to expect that the presence of the diffuser walls will not influence the flow through the exhaust nozzle because no pressure disturbances downstream of the nozzle could be transmitted upstream past the nozzle outlet. Inasmuch as no interference effects were found at the ram-pressure ratio of 1.0 and, as reasonable assurance exists that no interference is present at the very high ram-pressure ratios, performance is probably accurately obtained at the intermediate values of ram-pressure ratios.

Pressure Measurements in Exhaust Chamber

A further indication that the presence of the jet diffuser did not interfere with the flow through the exhaust nozzle at ram-pressure ratios greater than 1.0 was obtained from the pressure surveys in the exhaust chamber. Because any interference effects would be manifested in an uneven pressure distribution in the exhaust chamber, the small magnitude of the pressure variations shown in the typical pressure distribution of figure 18 indicates

that no appreciable interference effects were present. Furthermore,
the difference between the various pressures in the exhaust chamber
and the pressure p_8 used as the effective pressure acting on the
diaphragm seal during the runs was less than 4 inches of water.
These small pressure variations could be responsible for only about
10 pounds error in the thrust calibration.

SUMMARY OF RESULTS

With a jet diffuser developed to simulate ram-pressure and
altitude conditions on a turbojet-engine static test stand, a
maximum simulated ram-pressure ratio (engine-inlet to exhaust-
chamber pressure ratio) of about 2.4 was obtained at a simulated
pressure altitude of approximately 23,000 feet.

Part of the pressure rise between the exhaust chamber and the
atmosphere occurred between the exhaust chamber and the diffuser-
throat outlet and this pressure rise was in good agreement with a
theoretical analysis. The analysis also showed that an optimum
diffuser-throat area existed. The optimum area ratio was dependent
upon the ratio of jet thrust to the product of the ratio of specific
heats of the exhaust gas, exhaust-chamber ambient pressure, and
engine-exhaust-nozzle outlet area, F_j/p_8A_n. The existence of an
optimum throat area was confirmed by experimental data for diffuser-
throat diameters of $13\frac{1}{2}$ and 14 inches.

The good agreement of performance data at a ram-pressure ratio
of 1.0 obtained with and without the jet diffuser indicated that
the presence of the jet diffuser did not interfere with the flow
through the engine exhaust nozzle at this ram-pressure ratio. The
small pressure gradients measured in the exhaust chamber indicated
that the presence of the jet diffuser had no effect on jet thrust
at the high ram-pressure ratios.

Flight Propulsion Research Laboratory,
    National Advisory Committee for Aeronautics,
        Cleveland, Ohio, October 10, 1947.

APPENDIX A - DERIVATION OF EQUATION FOR PRESSURE RISE

BETWEEN STATIONS 8 AND 9

The ideal pressure rise between stations 8 and 9 may be calculated by use of the fundamental equations of conservation of energy, momentum, and mass flow and the gas law. The following preliminary assumptions are made: (a) Velocity is uniform at stations 8 and 9; and (b) friction or separation losses along the walls of the throat are negligible. The momentum equation may be written between stations 8 and 9 as

$$\frac{W_t}{g} V_9 + p_9 A_9 = \frac{W_t}{g} V_j + p_8 A_9 \tag{3}$$

which is the momentum equation for flow through the sudden expansion.

The jet thrust is given by

$$F_j = \frac{W_t}{g} V_j \tag{4}$$

Combining equations (3) and (4) gives

$$(p_9 - p_8) A_9 = F_j - \frac{W_t}{g} V_9 \tag{5}$$

If the increase in area of the jet due to free expansion for the conditions of moderately supersonic jet velocities is neglected, the continuity equation may be written

$$W_t = \rho_j A_n V_j = \rho_9 A_9 V_9$$

and

$$V_9 = \frac{\rho_j}{\rho_9} \frac{A_n}{A_9} V_j \tag{6}$$

The assumption that the increase in area of the jet may be neglected at moderately supersonic jet velocities was checked at an exhaust-gas Mach number of 1.4. The increase in jet area due to free expansion was found to change the ideal pressure ratio p_9/p_8 less than 1 percent.

By substitution of V_j from equation (4) in equation (6)

$$V_9 = g \frac{\rho_j}{\rho_9} \frac{A_n}{A_9} \frac{F_j}{W_t}$$ (7)

Eliminating V_9 from equation (5) by substituting equation (7) gives

$$(p_9 - p_8) A_9 = F_j \left(1 - \frac{A_n}{A_9} \frac{p_8}{p_9} \frac{t_9}{t_j}\right)$$ (8)

The equation for conservation of energy between stations 8 and 9 may be written

$$\frac{V_j^2}{2g} + \frac{\gamma}{\gamma-1} R t_j = \frac{V_9^2}{2g} + \frac{\gamma}{\gamma-1} R t_9$$ (9)

When equation (9) is expressed in terms of temperature ratio, and when t_9/t_j, V_9, and V_j are eliminated in equations (4), (6), (8), and (9), and when the resulting equation is combined with the gas law, the final equation may be written

$$\frac{F_j}{\gamma p_8 A_n} = \frac{1 + \frac{2}{\gamma-1} \frac{p_9}{p_8} - \frac{\gamma+1}{\gamma-1} \left(\frac{p_9}{p_8}\right)^2}{\frac{2\gamma^2}{\gamma-1} \left(\frac{A_n}{A_9}\right)^2 - 2\gamma \left(\frac{A_n}{A_9}\right) - \frac{2\gamma}{\gamma-1} \frac{p_9}{p_8} \left(\frac{A_n}{A_9}\right)}$$ (1)

It should be noted that

$$M_j^2 = \frac{F_j}{\gamma p_8 A_n}$$

REFERENCE

1. Sanders, Newell D.: Performance Parameters for Jet-Propulsion Engines. NACA TN No. 1106, 1946.
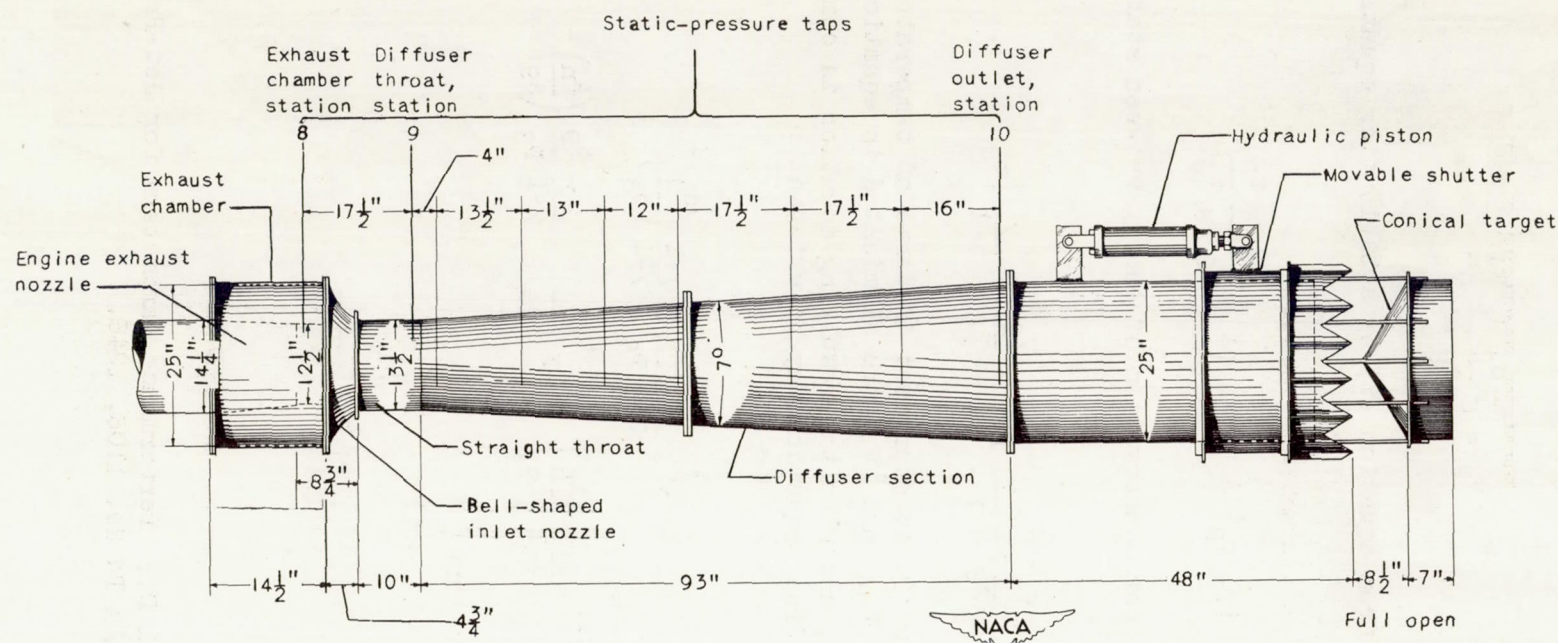
Figure 1. – Diagram of jet-diffuser assembly for turbojet engine with a 12½-inch-diameter exhaust-nozzle outlet showing location of pressure taps. (Additional static-pressure taps in exhaust chamber, inlet nozzle, and throat are shown in fig. 3).
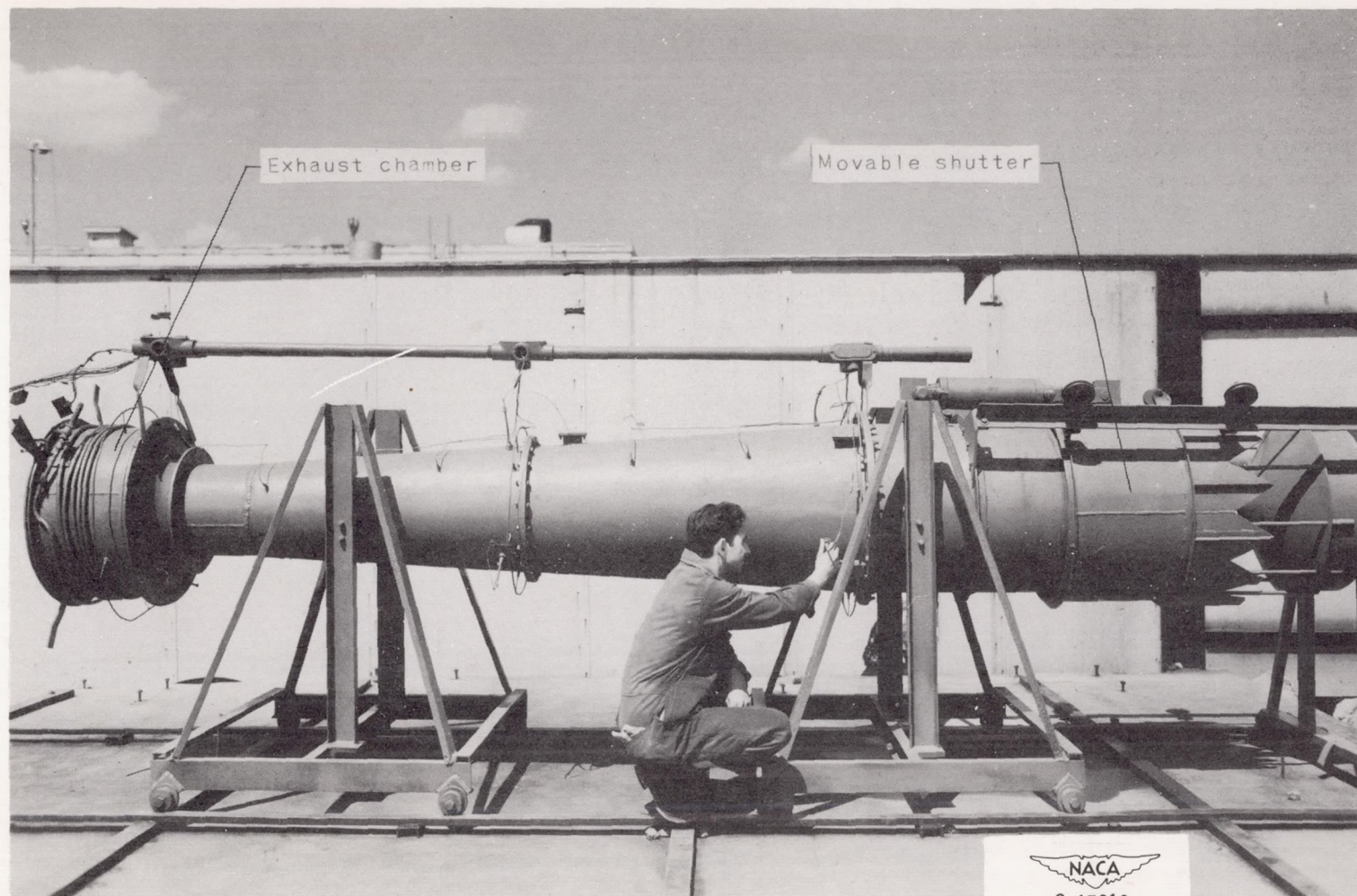
Figure 2. - Jet diffuser mounted on movable frame.
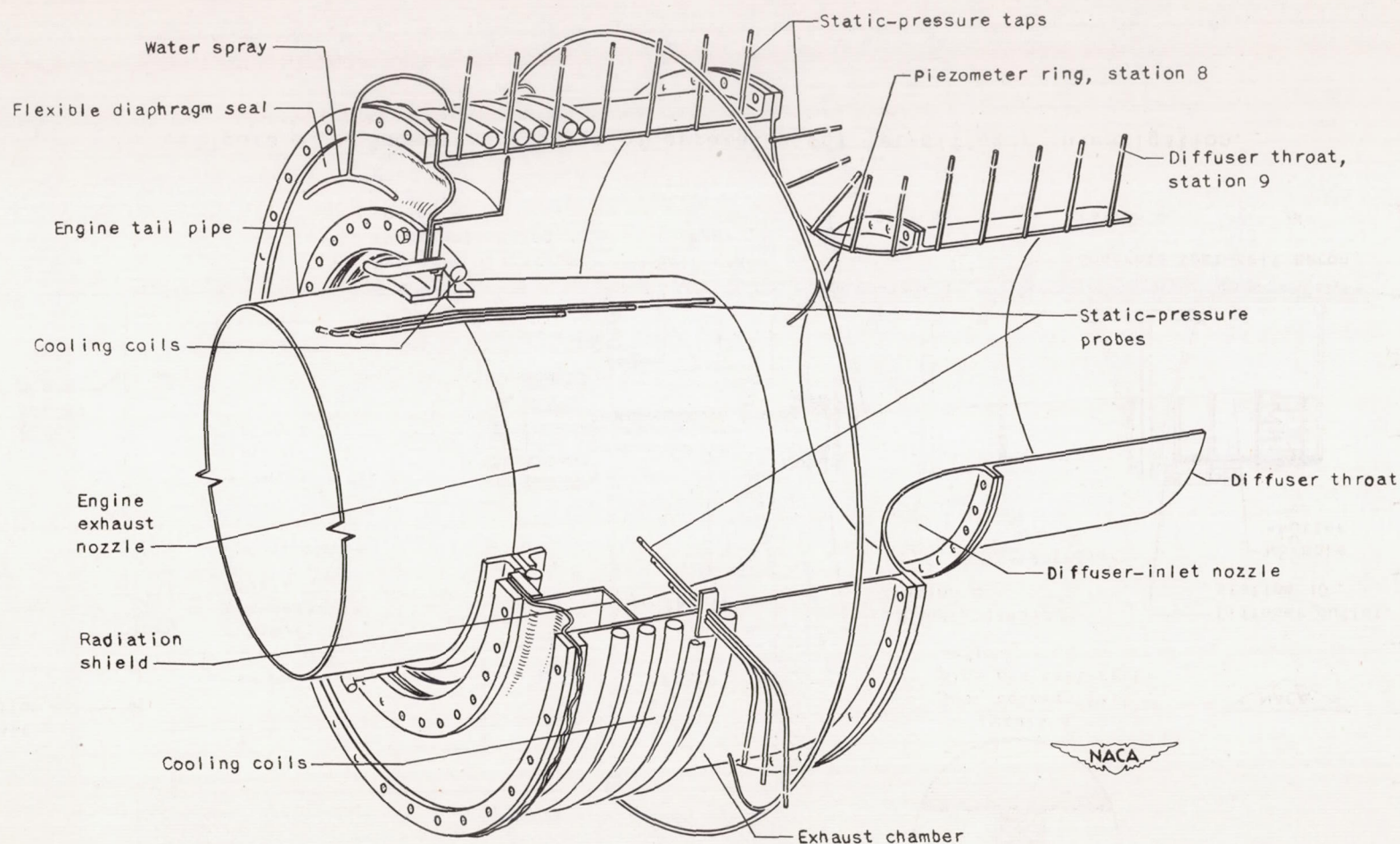
Figure 3. – Cutaway sketch of jet–diffuser exhaust chamber showing location of pressure-measuring stations.

Air
flow →

Tail pipe ⎯
Steel wool ⎯

Detail A
Seal between tail
pipe and test-cell
wall

NACA

⎯ Standard
A.S.M.E.
air-metering
nozzle

⎯ Air-supply
diffuser

Tail
pipe,
station 7 ⎯

See detail A ⎯

⎯ Exhaust chamber,
station 8

⎯ Diffuser outlet,
station 10

Engine cowl ⎯

⎯ Jet diffuser

⎯ Movable
shutter

Compressor
inlet,
station 1 ⎯

Air-
sealed
doors ⎯

Suspended
frame ⎯

Balanced-diaphragm ⎯
thrust-measuring
device

⎯ Bell-crank
linkage

⎯ Diffuser throat, station 9

⎯ Concrete test-cell apron

Figure 4. — Schematic diagram of apparatus for jet-diffuser investigation.
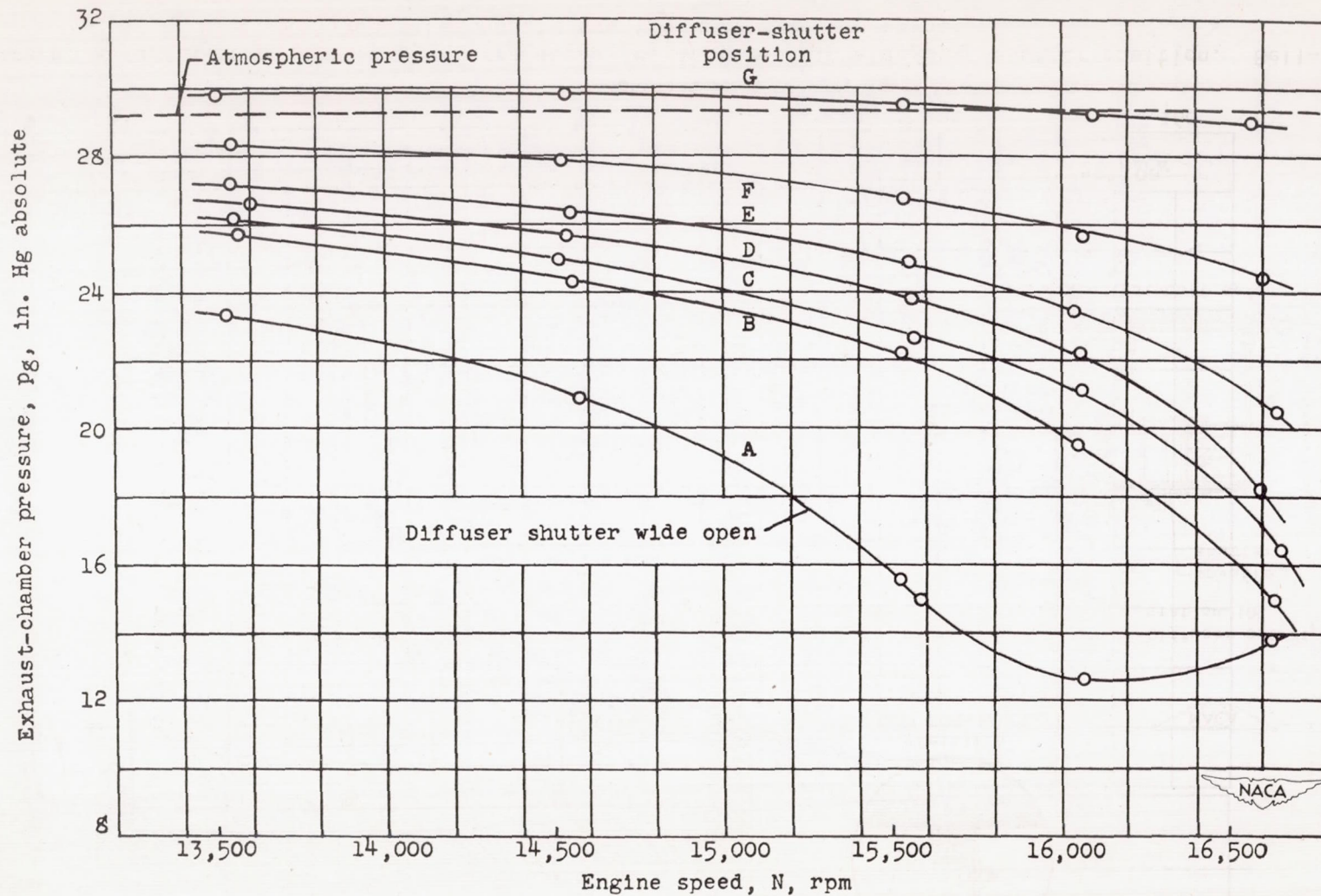
Figure 5. – Variation of exhaust-chamber pressure with engine speed for various shutter positions. Bell-shaped inlet nozzle and $13\frac{1}{2}$-inch-diameter throat.
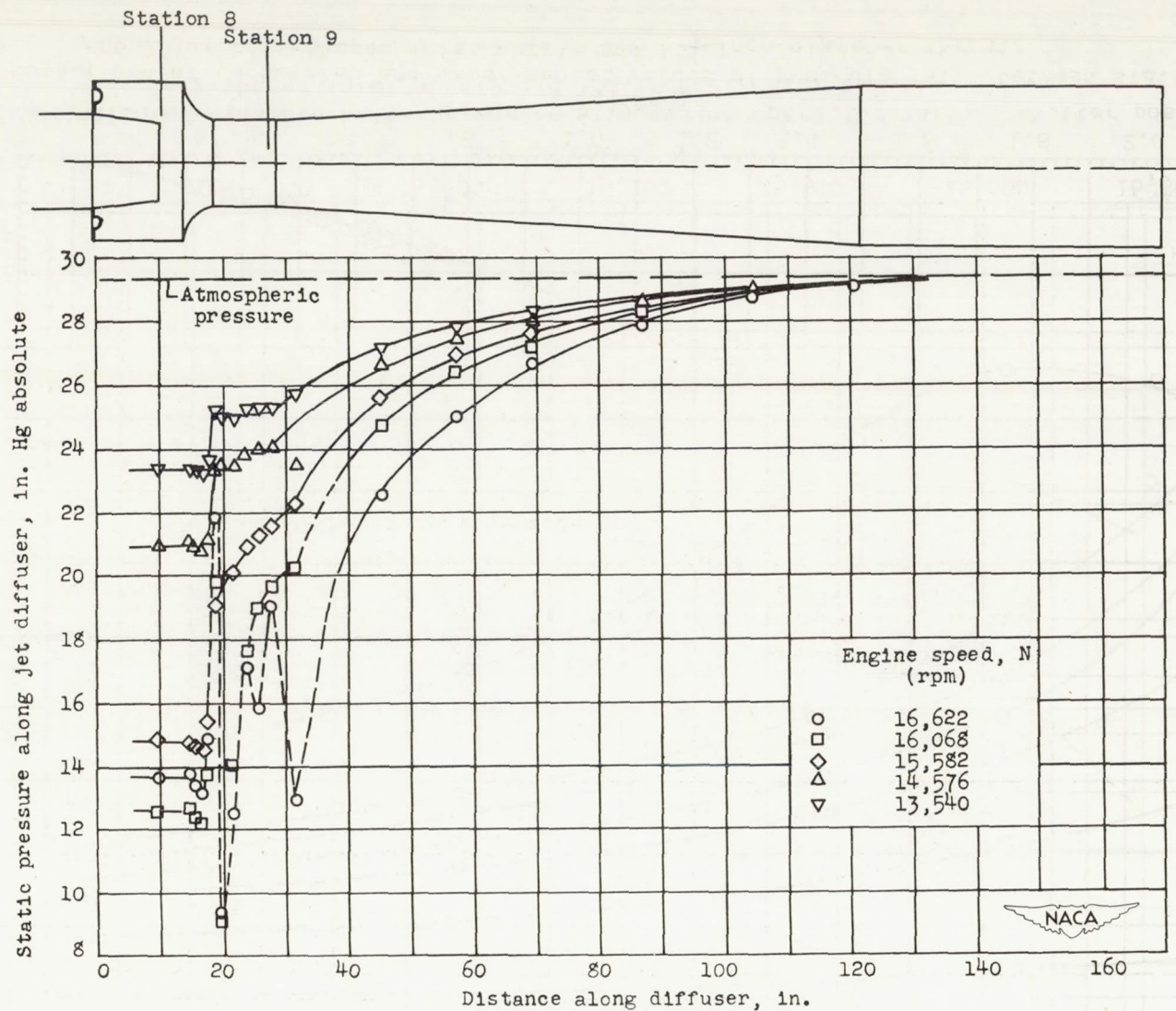
Figure 6. – Variation of static pressures along jet diffuser for wide-open shutter position. Bell-shaped inlet nozzle and $13\frac{1}{2}$-inch-diameter throat.
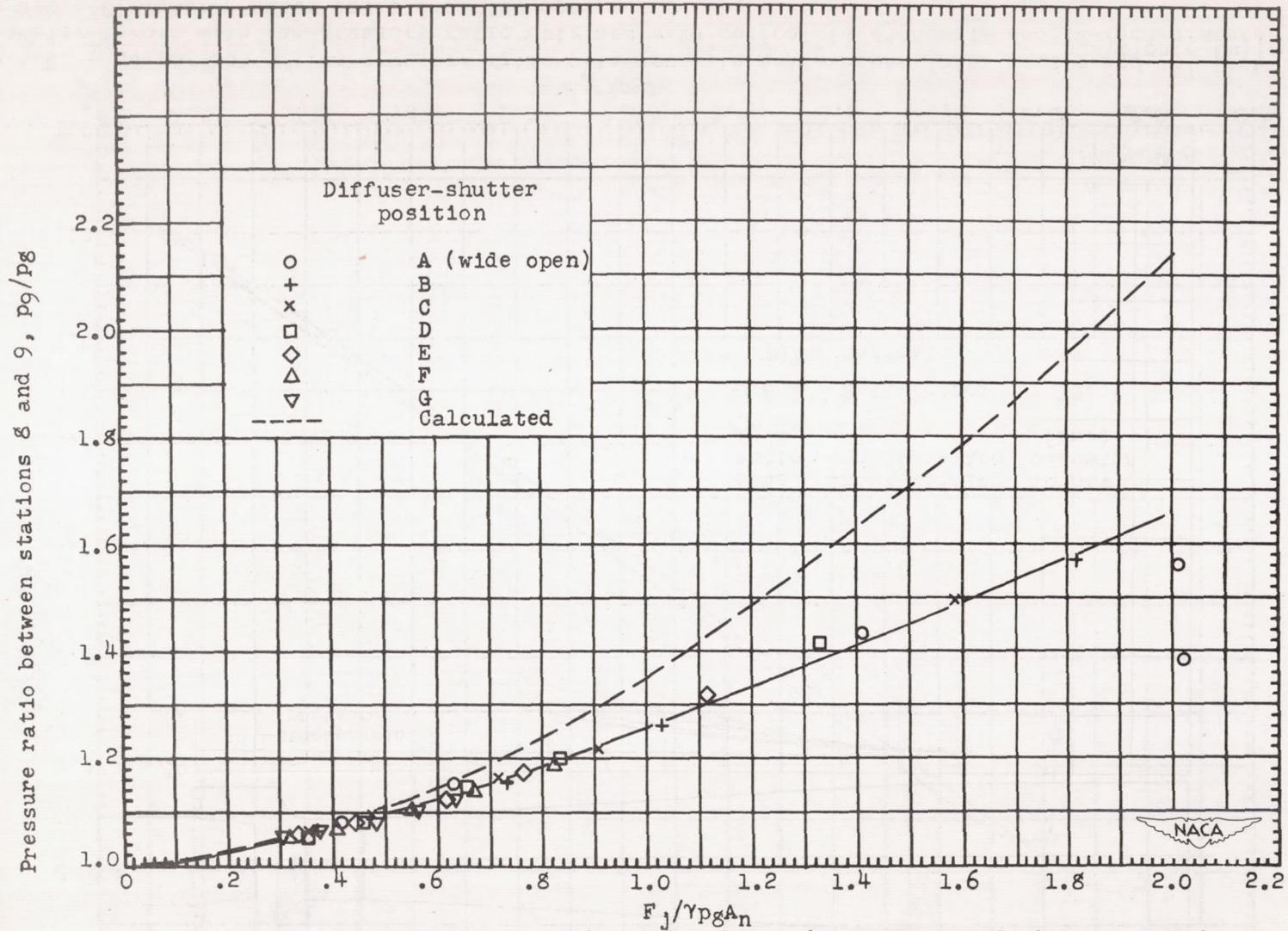
Figure 7. – Comparison of calculated and experimental values of pressure ratio between stations 8 and 9 for bell-shaped inlet nozzle and $13\frac{1}{2}$-inch-diameter throat.
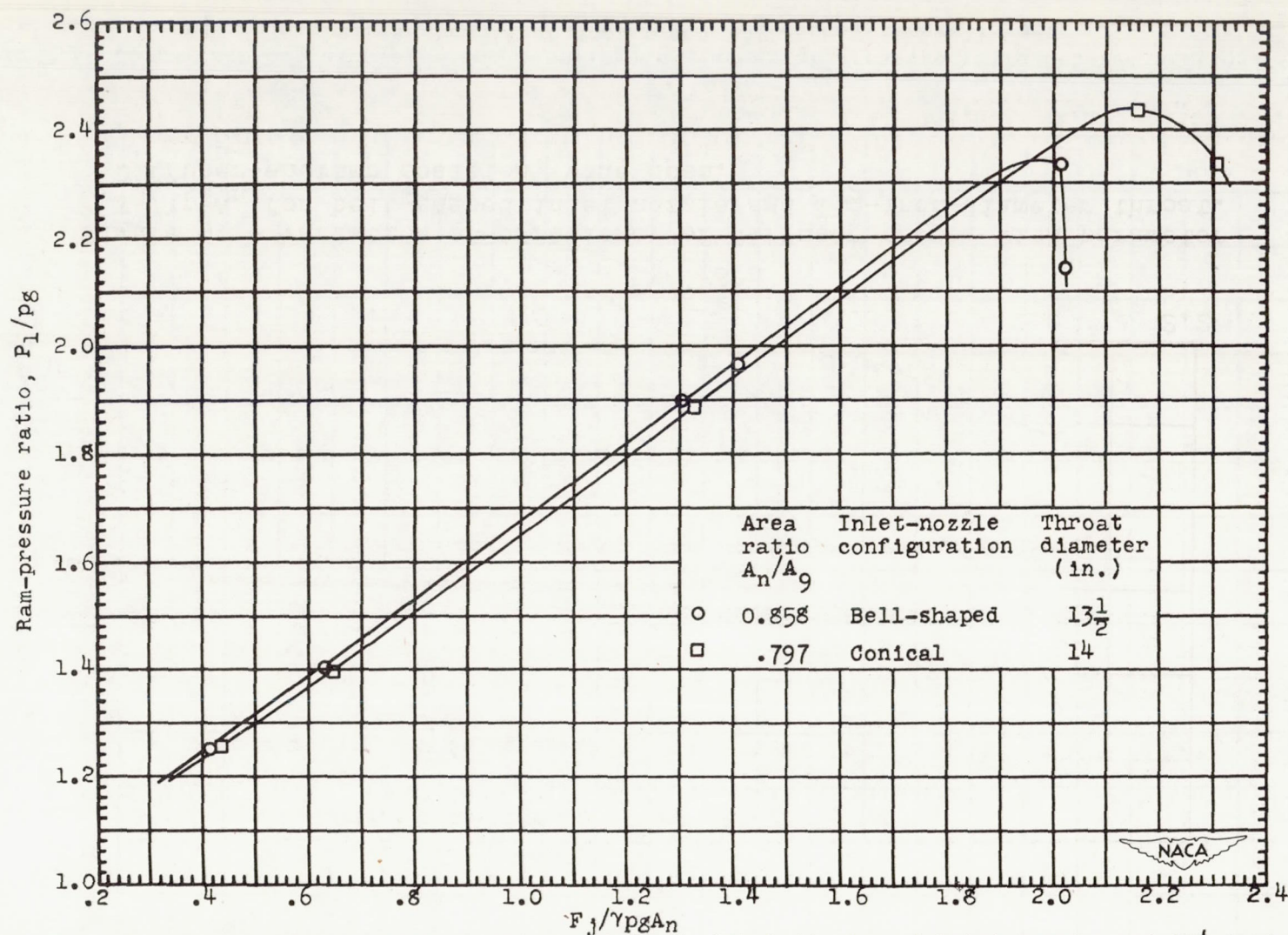
Figure 8. – Comparison of ram–pressure ratio obtained with bell–shaped inlet nozzle and $13\frac{1}{2}$–inch–diameter throat with ram–pressure ratio obtained with conical inlet nozzle and 14–inch–diameter throat.   Diffuser–shutter position, wide open.
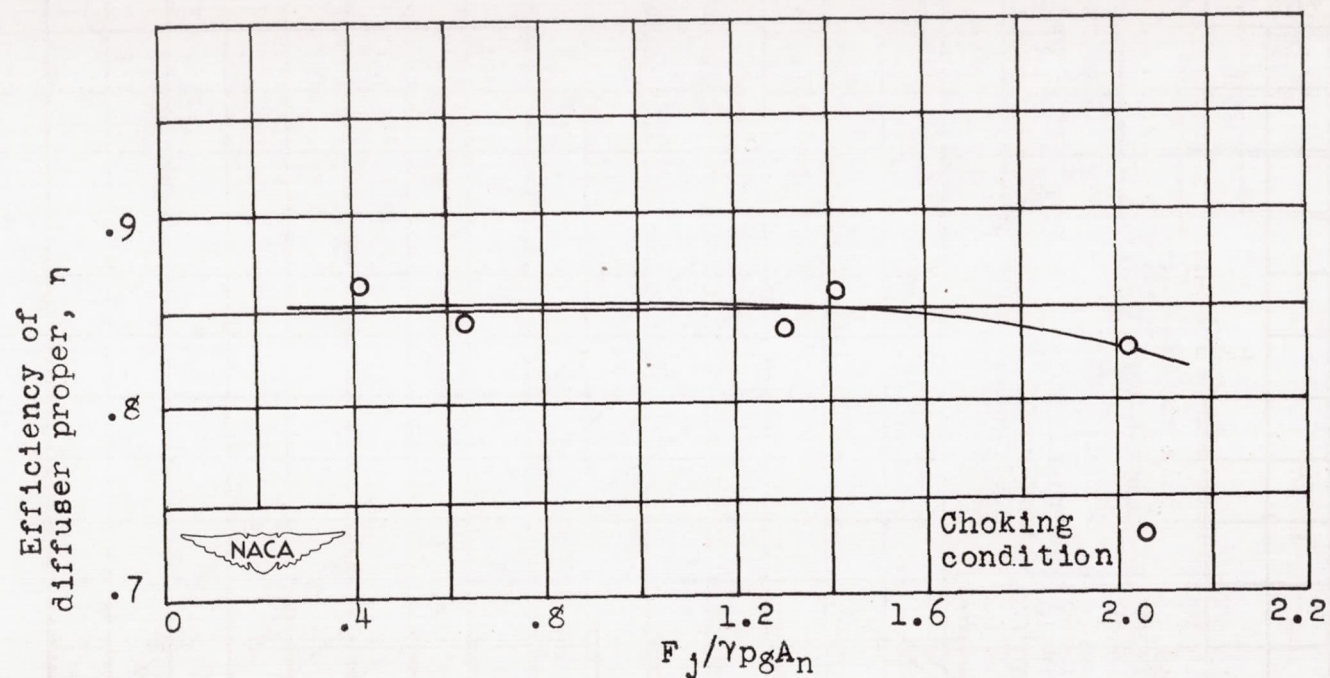
Figure 9. – Variation of efficiency of diffuser proper with parameter $F_j/\gamma pgA_n$ for bell-shaped inlet nozzle and $13\frac{1}{2}$-inch-diameter throat. Diffuser-shutter position, wide open.
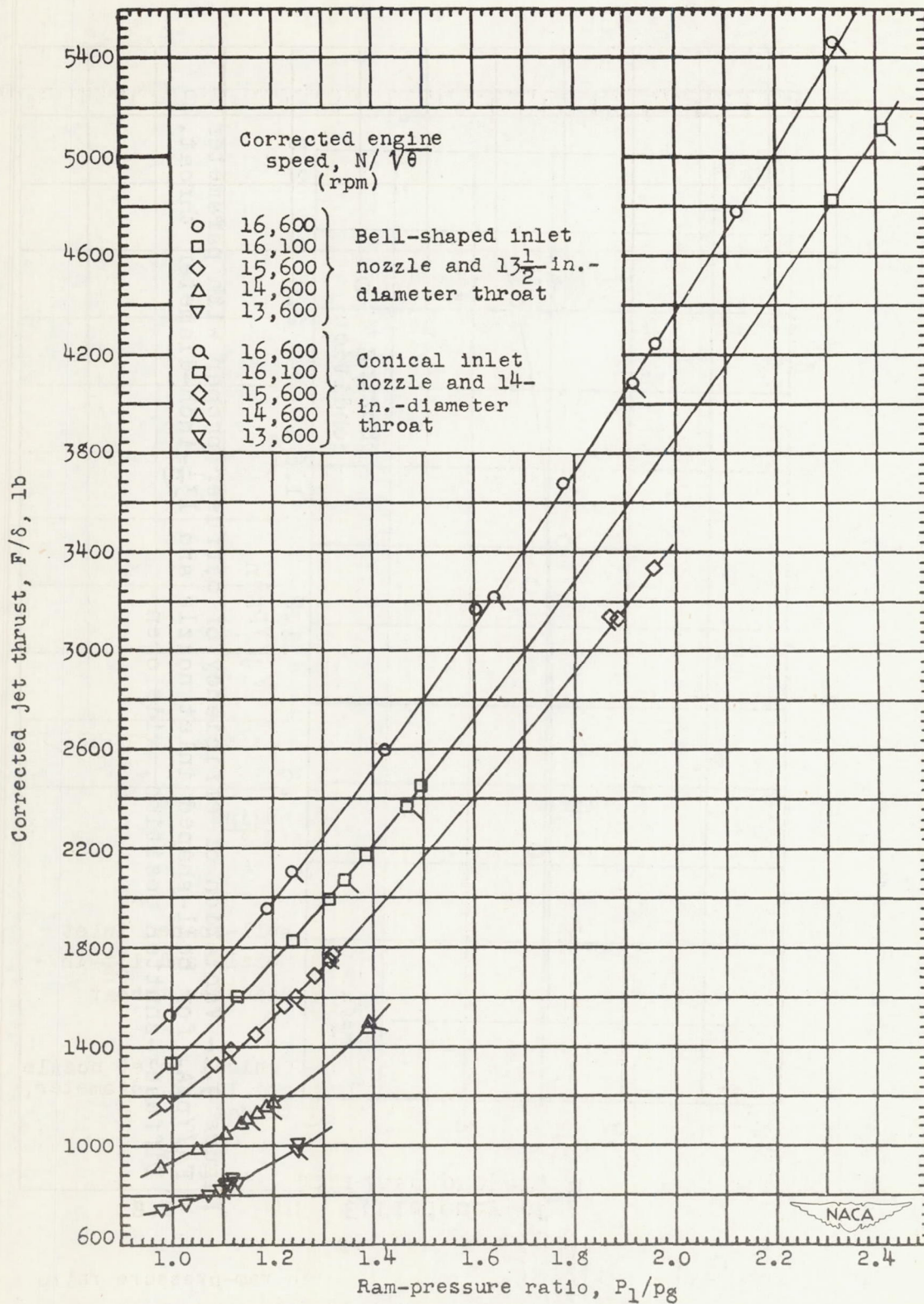
Figure 10. — Variation of corrected jet thrust with ram-pressure ratio for various corrected engine speeds.
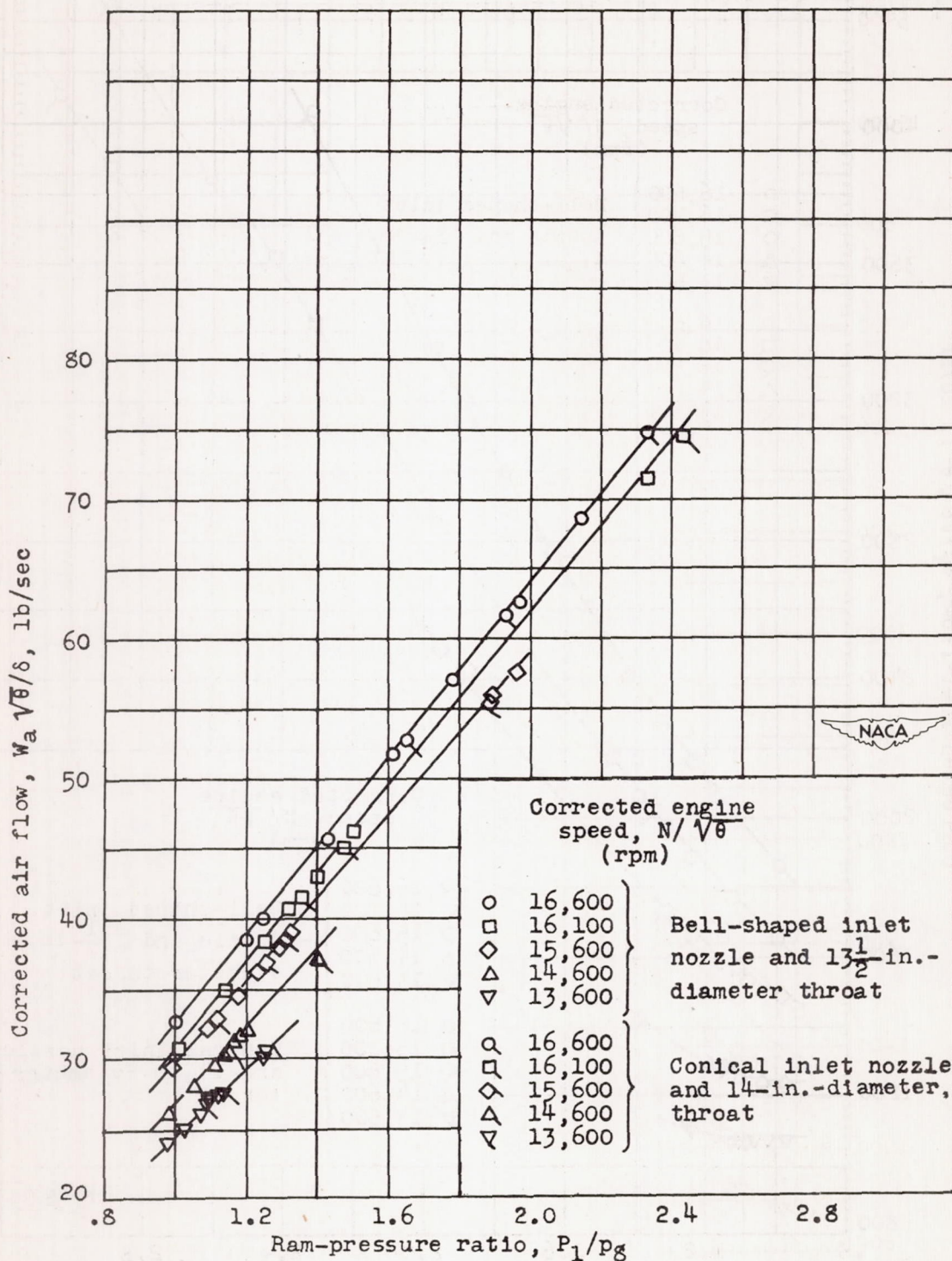
Figure 11. — Variation of corrected air flow with ram-pressure ratio for various corrected engine speeds.
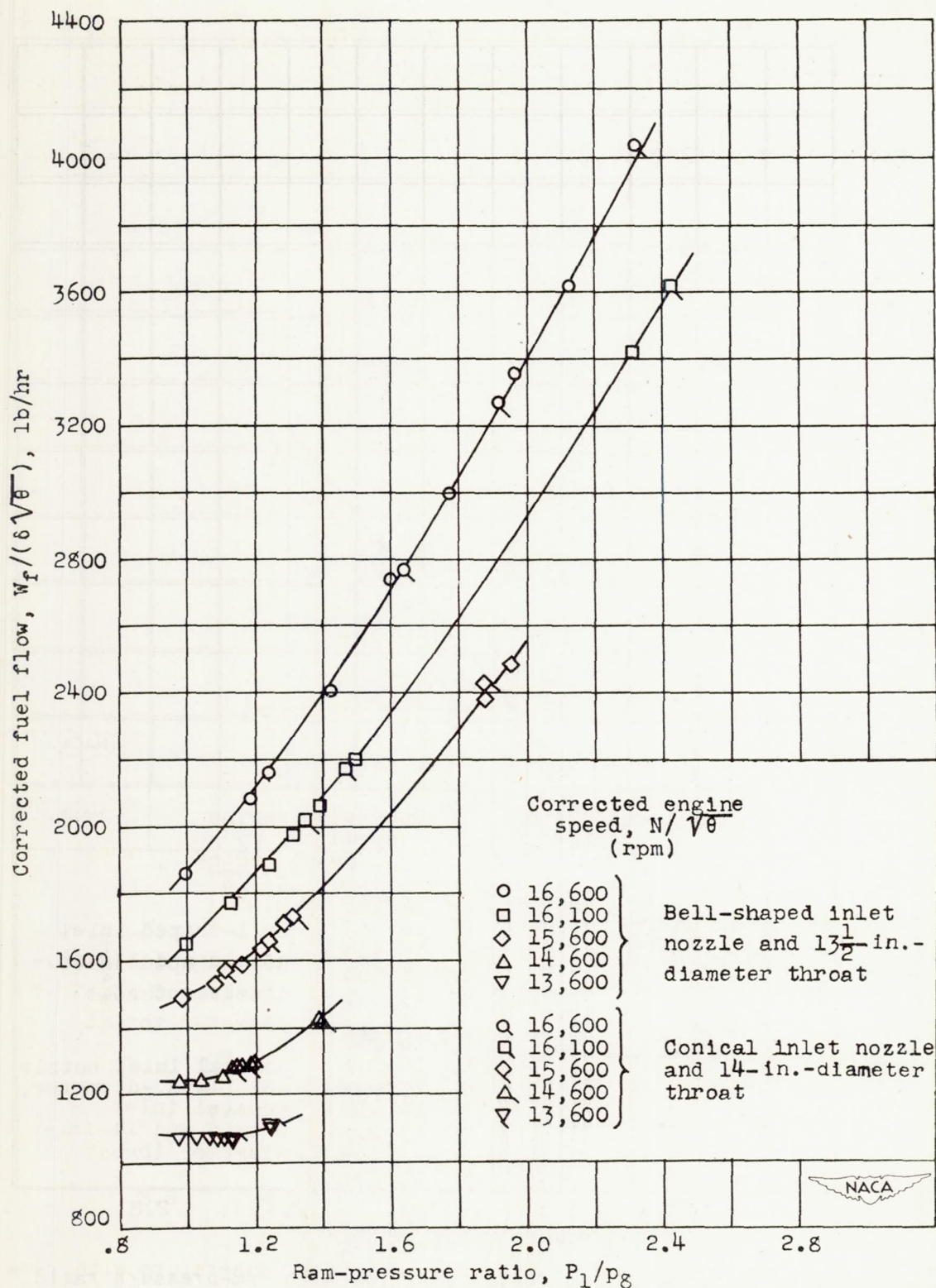
Figure 12. – Variation of corrected fuel flow with ram-pressure ratio
for various corrected engine speeds.
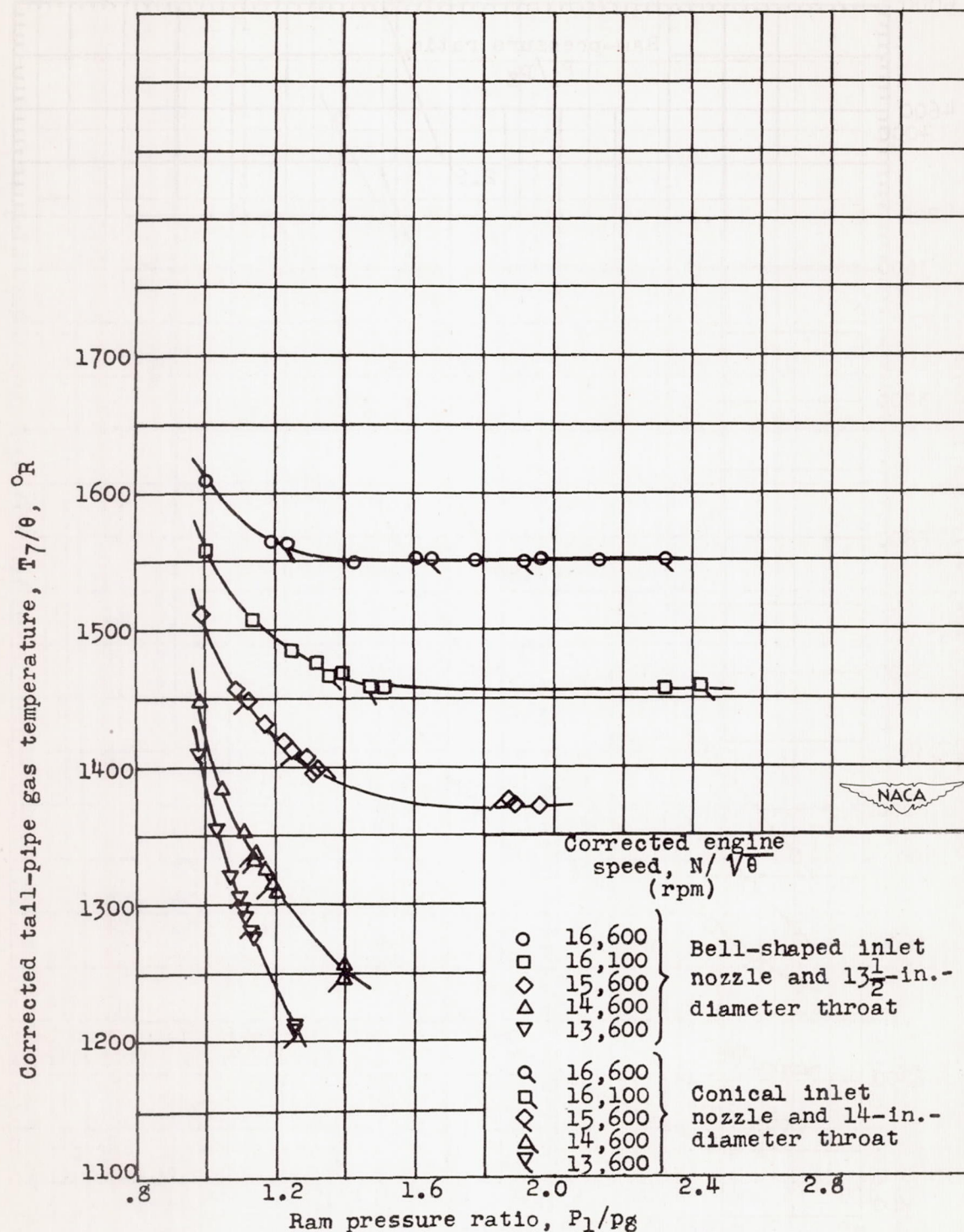
Figure 13. – Variation of corrected tail-pipe gas temperature with ram-pressure ratio for various corrected engine speeds.
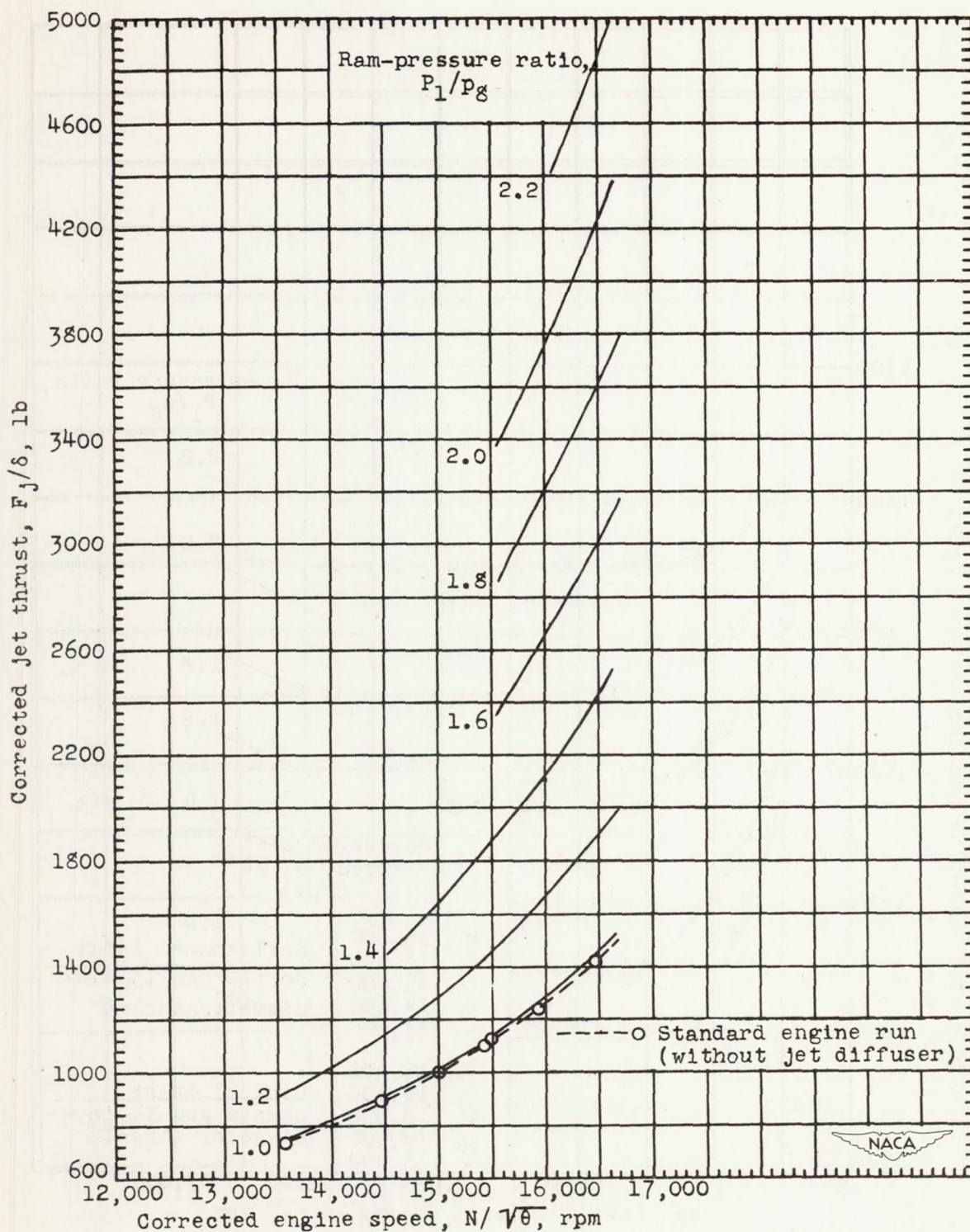
Figure 14. — Variation of corrected jet thrust with corrected engine
speed for various ram-pressure ratios.

678
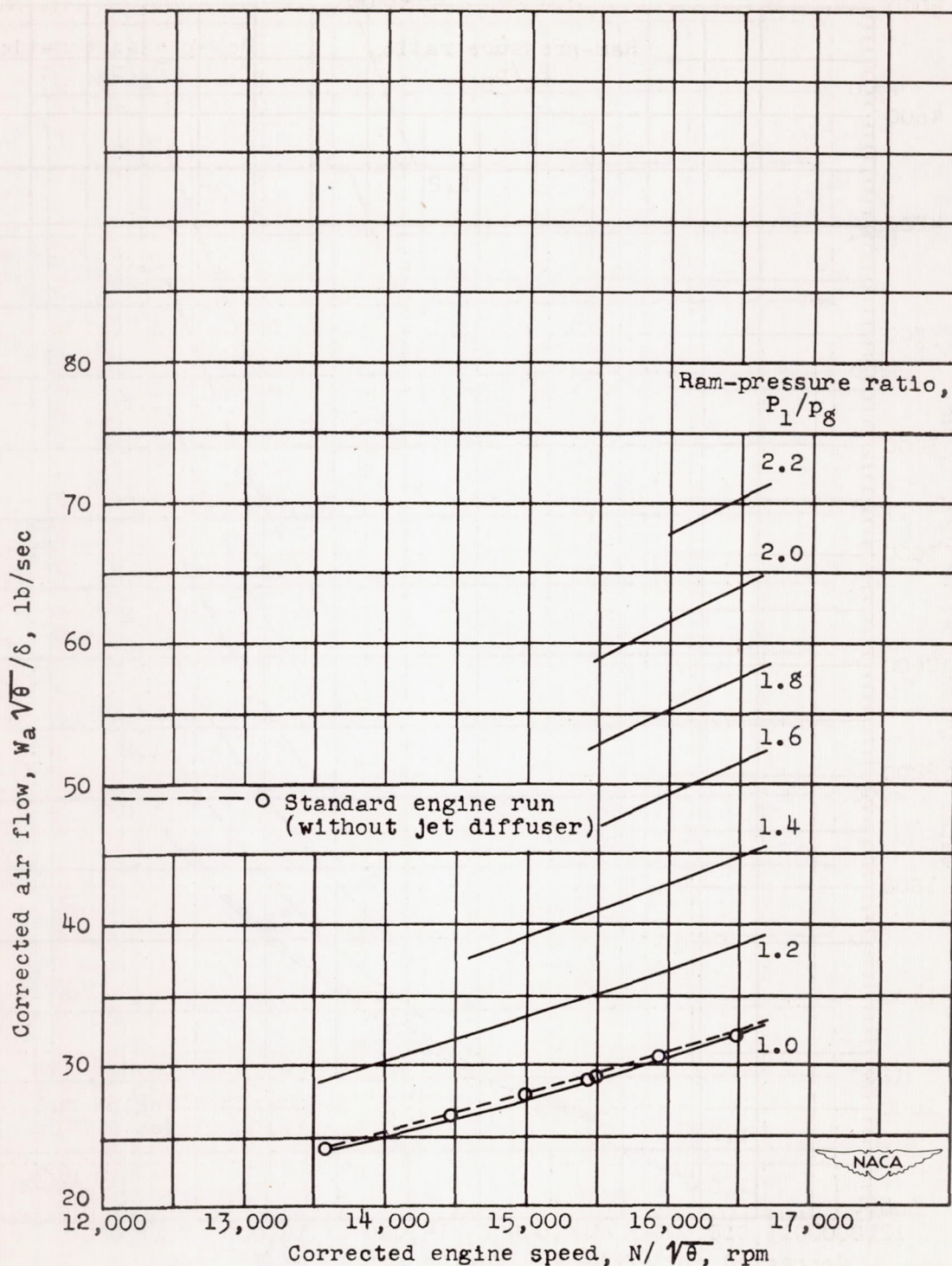
Figure 15. – Variation of corrected air flow with corrected engine speed for various ram-pressure ratios.
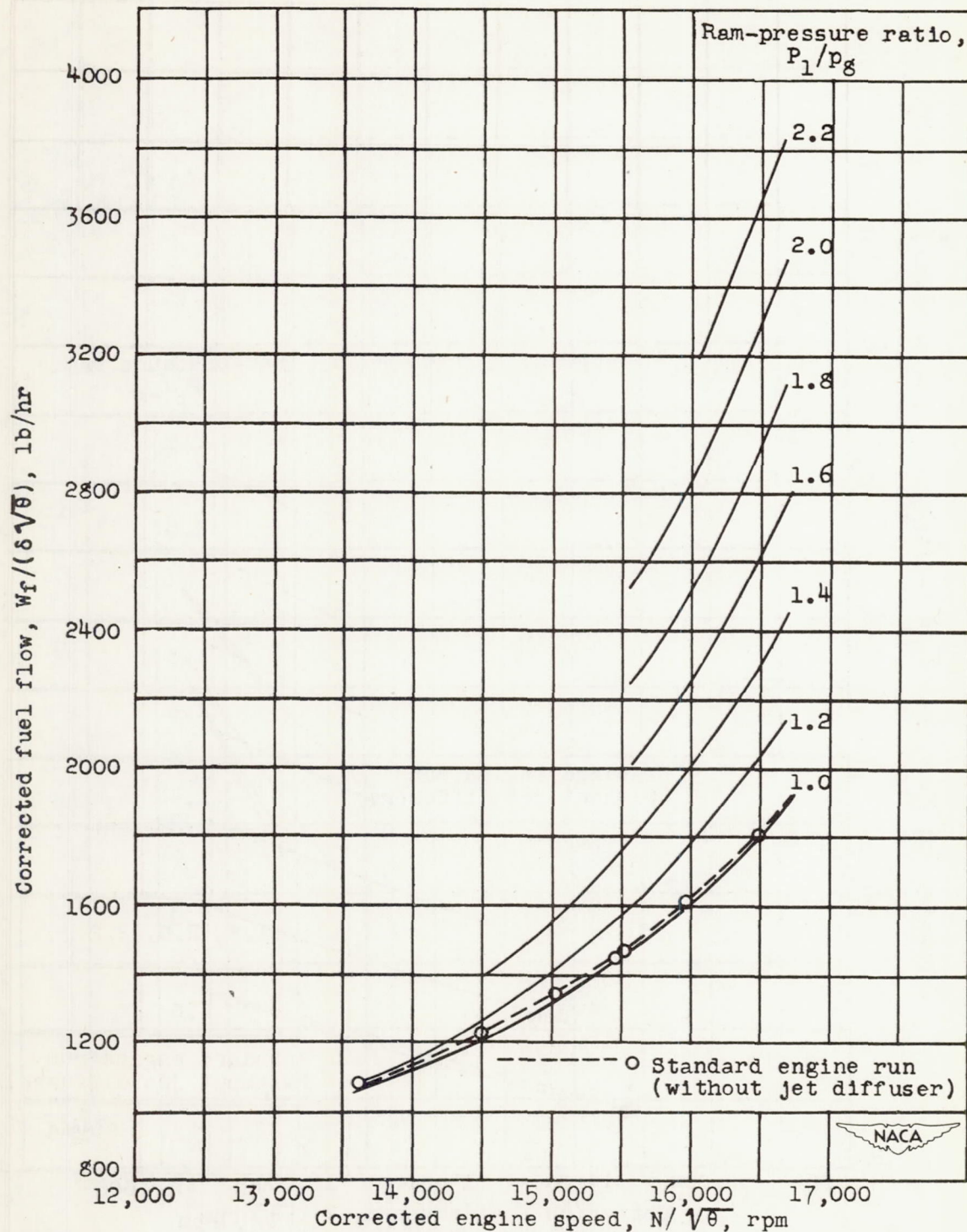
Figure 16. — Variation of corrected fuel flow with corrected engine
speed for various ram-pressure ratios.
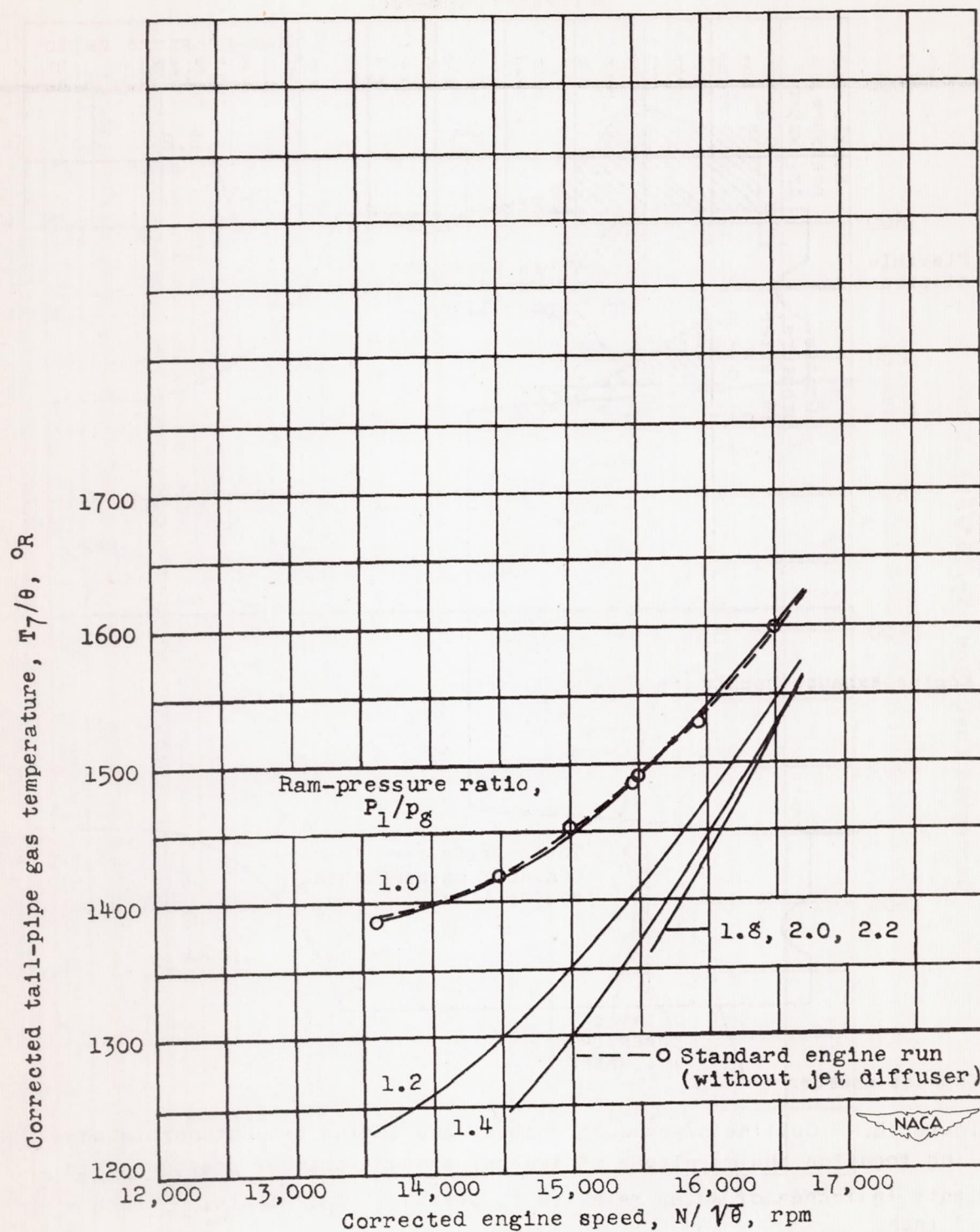
Figure 17. – Variation of corrected tail-pipe gas temperature with corrected engine speed for various ram-pressure ratios.

Static pressure, in. water

p_g

Flexible
diaphragm

These pressures
measured on vertical
center lines

Static pressure, in. water

Engine-exhaust nozzle

These pressures
measured on horizontal
center line

Static
pressure,
in. water
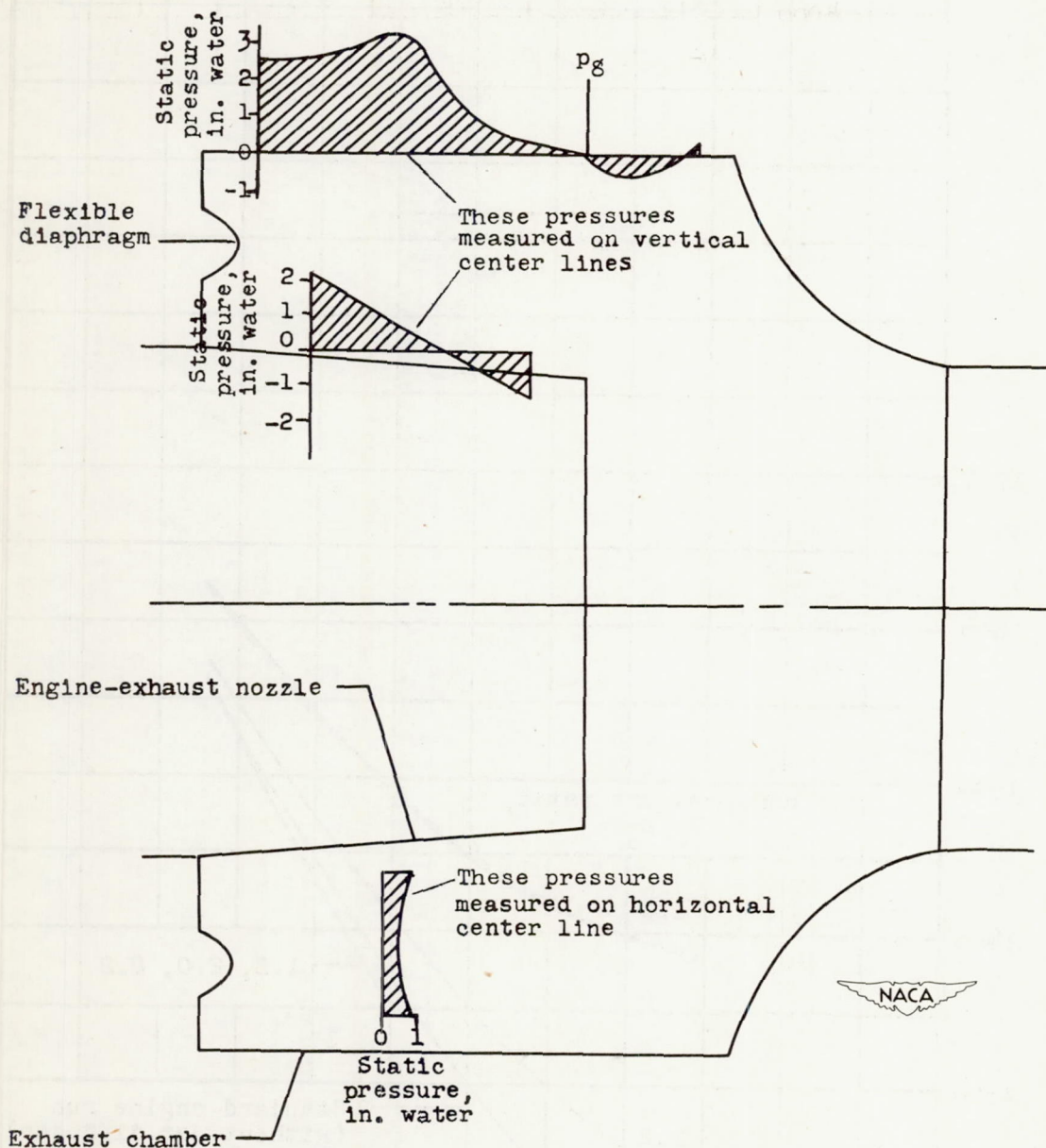
Exhaust chamber

Figure 18. – Outline of exhaust chamber and engine exhaust nozzle show-
ing location and magnitude of typical exhaust-chamber pressure gradi-
ents in inches of water relative to pressure p_g. Scale: $\frac{1}{4}$ inch =
1 inch.